



**“Gheorghe Asachi” Technical University of Iasi, Romania**



## STUDIES ON THE PHOTOCATALYTIC DEGRADATION OF ORGANIC DYES USING CeO<sub>2</sub> - ZnO MIXED OXIDES

**Gabriela Antoaneta Apostolescu, Corina Cernatescu, Claudia Cobzaru, Ramona Elena Tataru-Farmus, Nicolae Apostolescu\***

*“Gheorghe Asachi” Technical University of Iasi, Faculty of Chemical Engineering and Environmental Protection, 73 Prof. Dr. docent Dimitrie Mangeron Str., 700050 Iasi, Romania*

### Abstract

A new catalytic mixture of nanosized dioxide (CeO<sub>2</sub>) and zinc oxide (ZnO) powders have been synthesized by surfactant-assisted solvo-thermal route, characterized and evaluated for photocatalytic activity. The prepared catalysts were characterized by TG, XRD, SEM and EDAX methods. SEM analysis showed that the catalyst particles have spheroidal shape and their sizes range from 50 to 80 nm, organised as uniform distributed aggregates with large surface area, leading to the existence of a large number of defects. The photocatalytic activity of these materials was evaluated by UV-Vis spectroscopy for degradation of methylene blue (MB) and 4'-(1-methyl-benzimidazol-2"-phenylazo-2"-8"-amino-1"-hydroxy-3",6"-disulphonic)-naphthalene acid (PMBH) in water.

*Key words:* CeO<sub>2</sub> - ZnO mixed oxides, MB, organic dye photodegradation

*Received:* November, 2014; *Revised final:* February, 2015; *Accepted:* February, 2015

### 1. Introduction

Materials based on mixed oxide (CeO<sub>2</sub> - ZnO) nano-powders have been intensive studied in the last years in order to find the best solutions to improve or to fix some environmental problems (Faisal et al., 2013; Lima et al., 2009; Nascimento et al., 2014). Separately, cerium oxide (simple or in matrix) is used as catalyst or catalyst support material, in optical devices as semiconductor or as gas sensor (Ghodsi et al., 2008; Paul et al., 2008; Preetam and Hegde, 2008), and recently have appeared studies about antiseptic properties or UV filter in sunscreen. Also, zinc oxide (simple or in matrix) is studied for its applications as semiconductor, pigment, antiseptic or in sunscreens (Ameen et al., 2012; Ezenwa, 2010; Kashif et al., 2013; Shafaei et al., 2010). Both materials show properties that can be easily exploited. Therefore, it is interesting to study the

behaviour of the material obtained by combining in specific conditions of these two oxides.

Due to the last trends in environmental protection it is required to find some new materials that could be used to purify exhausted waters, mainly the organic compounds well known to be toxic. The degradation of organic compounds produced in industrial processes using the most efficient methods and advanced materials has emerged as a necessity to protect the environment (Arsene et al., 2013). Following this trend, the degradation of organic effluents have been studied by using various catalytic materials based on cerium / zinc oxide simple or doped with various metals or materials.

Studies are reported on photocatalytic degradation of methylene blue dye, Rhodamine B, methyl tert-butyl ether, castor oil or other organic compounds (Abbas et al., 2014; Akyol et al., 2005; Bansal and Sud, 2011; Fan et al., 2008; Khataee et

\* Author to whom all correspondence should be addressed: e-mail: [napostol@ch.tuiasi.ro](mailto:napostol@ch.tuiasi.ro)

al., 2015; Ko et al., 2014; Kumar et al., 2014; Orbeci et al., 2014; Shidpour et al., 2014; Wang et al., 2009).

Our research is focused on the development of efficient and inexpensive smart materials that can be used in several areas of heterogeneous catalysis, such as the combination of cerium oxide and zinc oxide that generates good results. This material is correlated with low price and low toxicity of zinc oxide that recommend it as promising photocatalyst. Also the possibilities of modelling the structural and textural properties of synthesized catalyst can contribute to the improvement of the photocatalytic activity.

## 2. Materials and methods

All chemicals used in this study were of analytical grade and used without further purifications. The starting materials were  $\text{Ce}_2(\text{C}_2\text{O}_4)_3 \cdot x\text{H}_2\text{O}$ ,  $\text{ZnC}_2\text{O}_4 \cdot x\text{H}_2\text{O}$  (all 99.99% purity, supplied from Aldrich), and PVA (average Mw 89,000 - 98,000, 99 %, Aldrich), ethanol and methylene blue (Chemical Company). The pH was adjusted with NaOH or HCl (Chemical Company). The 4'-(1-methyl-benzimidazolyl-2)-phenylazo-2''-(8''-amino-1''-hydroxy-3'',6''-disulphonic)-naphthalene acid, was synthesized in our laboratory. This compound is abbreviated as PMBH. A SP-870 plus METERTECH UV - Vis spectrophotometer was used to monitor the residue concentration of methylene blue (abbreviated as MB) and PMBH.

**Methylene blue** is a cationic dye with the structure shown in Fig. 1. It is most commonly used for colouring paper, temporary hair dye, dyeing cotton, wools and so on th. MB, although not considered to be a very toxic dye it can reveal very harmful effects on the living things.

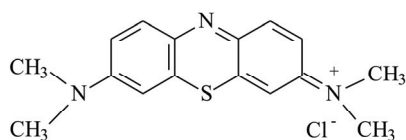


Fig. 1. Methylene blue structure

Methylene blue is a thiazinic dye and could be reduced by X and UV rays, acid pH or by using various salts as catalysts.

### 4'-(1-methyl-benzimidazolyl-2)-phenylazo-2''-(8''-amino-1''-hydroxy-3'',6''-disulphonic)-naphthalene acid (PMBH)

The PMBH ( $\text{C}_{24}\text{H}_{19}\text{N}_5\text{O}_7\text{S}_2$ ,  $M = 553\text{g/mol}$ , with the structure shown in Fig. 2) was synthesized in our laboratory, the synthesis being the subject of another paper, the structure of the azoic dye being presented below.

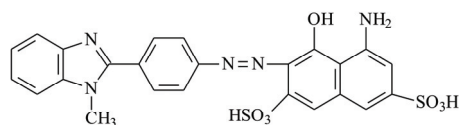


Fig. 2. 4'-(1-methyl-benzimidazolyl-2)-phenylazo-2''-(8''-amino-1''-hydroxy-3'',6''-disulphonic)-naphthalene acid structure

The reaction mixture was heated to  $150^\circ\text{C}$  and continuously stirred for 2 h, in a capped reactor and transferred into a 200 mL Teflon-lined autoclave. Then the autoclave was sealed and kept at  $160^\circ\text{C}$  for 8 h, and subsequently cooled down to room temperature naturally. The precipitate was separated by centrifugation (6000 rot/min, 5 min), washed three times with deionized water, and dried in vacuum at  $80^\circ\text{C}$  for 6 h. Finally, the product was calcined at  $450^\circ\text{C}$  in air for 4 h.

The final material obtained was a yellowish powder. The sample was examined by SEM (MIRA TESCAN and QUANTA 200 3D), EDAX (Quanta 200 3D electron microscope connected with EDS Ametek/EDAX equipment) thermal analysis (Pyris Diamond TG/DTA PerkinElmer), and XRD (Shimadzu XRD 6100 diffractometer using monochromatic  $\text{Cu K}\alpha$  radiation ( $\lambda = 0.154\text{ nm}$ ), operating at 40 kV and 30 mA).

### 3.2. Photocatalytic reaction procedure

The photocatalytic activity measurements were carried out as follows: the absorption mode of UV-Vis spectroscopy was used to measure the absorbance of various MB or PMBH concentration to plot the diagram of absorbance at 664 nm (in a.u., for MB) or 540 nm (in a.u., for PMBH) vs. concentration (mol/L). The reaction system containing 100 mL MB or PMBH aqueous solution with  $10^{-5}$  mol/L MB,  $5 \times 10^{-5}$  mol/L PMBH and 10 mg  $\text{CeO}_2 - \text{ZnO}$  photocatalyst was stirred magnetically in darkness at  $\text{pH}=7$ , for 30 min. To ensure a well dispersing and de-agglomeration of  $\text{CeO}_2 - \text{ZnO}$  nanopowder suspended in aqueous solution, a 400 W ultrasonic bath was used for 4 min. Before the irradiation, 3 mL of solution were taken out for adsorption analysis. The stirring was performed to reach the adsorption equilibrium of the MB/PMBH before exposure to UV irradiation from a 25 W Hg lamp. The distance between the lamp and reaction system was 5 cm and the temperature was set on  $25^\circ\text{C}$ . First, some experiments were done in two cases: in the presence of  $\text{CeO}_2 - \text{ZnO}$  photocatalyst and without any UV irradiation to identify the catalysis's influence and second, only under UV radiation to probe degradation of MB and PMBH solution.

For recording the first results without any light source, we put the prepared dispersed solution in a dark and cool place under vigorous stirring for 30 min. After beginning the irradiation process, the same amount of solution was taken out for each quantitative analysis, during 200 min. In these two cases there were no changes in the studied systems. A SP-870 plus METERTECH UV-Vis spectrophotometer was used to monitor the residue concentration of methylene blue and benzimidazole dye. All the photocatalytic experiments were repeated three times. The MB and PMBH removal was analysed by measuring the change in absorbance using UV-Visible spectrophotometer at 664 nm

corresponding to maximum absorption wavelength of MB and 540 nm for PMBH.

#### 4. Results and discussion

##### 4.1. Morphology and structure of $\text{CeO}_2$ - ZnO photocatalysts

The surface morphology, shape features and size determination of the synthesized  $\text{CeO}_2$  - ZnO nanocomposites were investigated using SEM and results are shown in Fig. 3 a-d, at different magnifications. In the first stage of organization can be observed association parallelepipedic crystals of about 2-5  $\mu\text{m}$  (images a, b). By increasing the magnification is observed the second level of organization, consisting of small spheroidal shape crystals, about 50-80 nm in diameter (images c, d). The agglomeration of nanocrystals is a commonly occurring phenomenon because the nanocrystals follow to decrease the exposed surface in order to minimize the interface energy.  $\text{CeO}_2$  - ZnO crystals have specific oriented aggregation of individual nanocrystals, leading to the existence of a large

number of defects. The X-ray patterns of and  $\text{CeO}_2$  - ZnO is depicted in Fig. 4. For  $\text{CeO}_2$  - ZnO nano powder, the reflection planes perfectly match the indexed  $\text{CeO}_2$ : cubic system and ZnO: hexagonal system. No peak due to any other phase was observed. In addition, the EDAX analysis (Fig. 5 and Table 1) indicate the presence of all components (Ce, Zn, O). The sharp peaks of Zn, Ce and O were obtained; no other peak related to any other element was detected in the spectrum within the detection limit which confirms that synthesized material composed of Zn, Ce and O only. The thermogravimetric (TG) and differential thermal analysis (DTA) were performed by using a Perkin-Elmer Pyris Diamond TG/DTA thermobalance which records simultaneously T, TG and DTA curves and are shown in Fig. 6 and Table 2. The DTG curves were obtained by numerical differentiation of the TG curves. The working conditions were as follows: sample mass 9.4 mg, heating rate 10  $^\circ\text{C min}^{-1}$ , temperature range 30 – 850  $^\circ\text{C}$  in air stream (80 mL  $\text{min}^{-1}$ ). There is no obvious weight change at above 420  $^\circ\text{C}$ , so that we chose that calcination occurs at 450  $^\circ\text{C}$ .

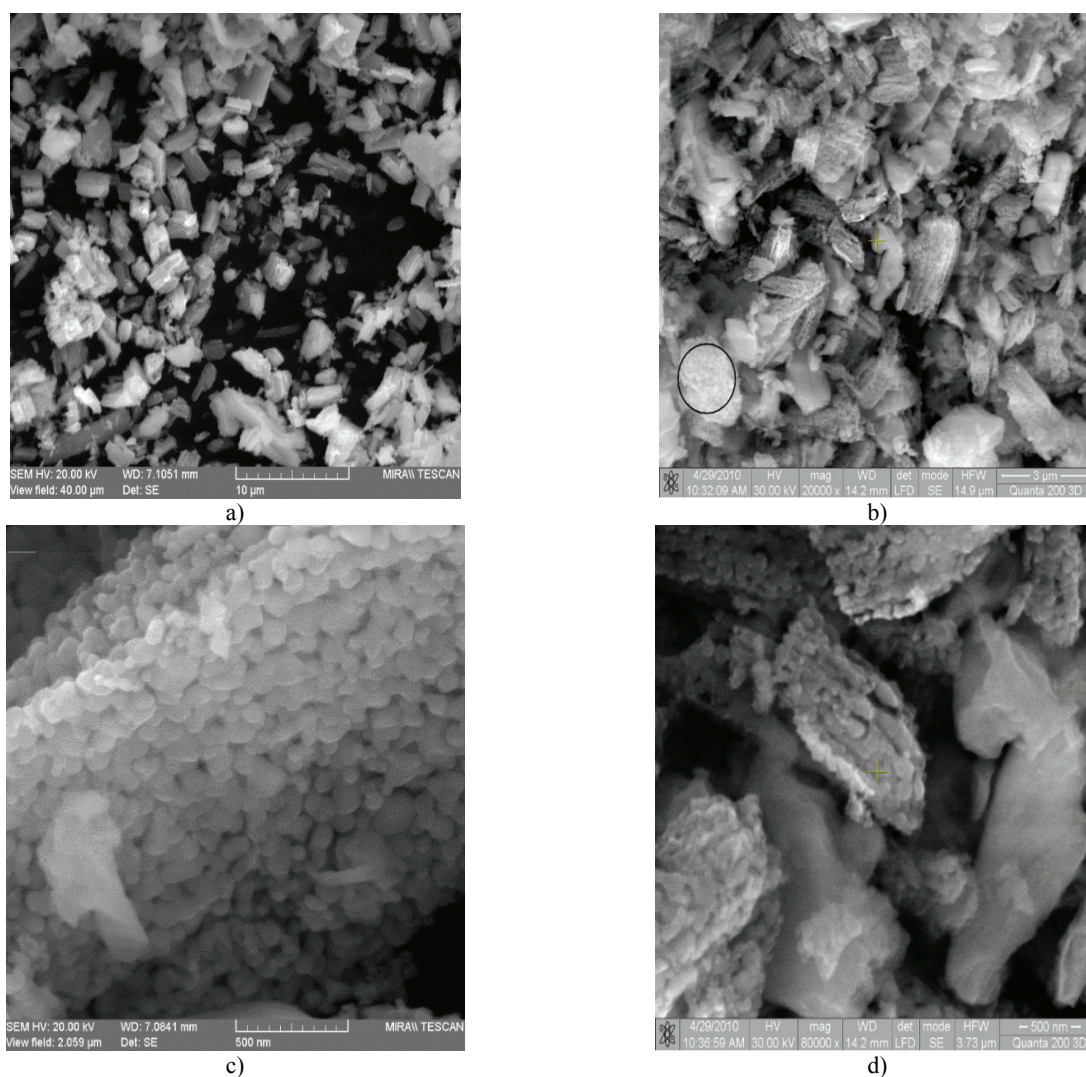


Fig. 3. The SEM images for  $\text{CeO}_2$  - ZnO synthesized material

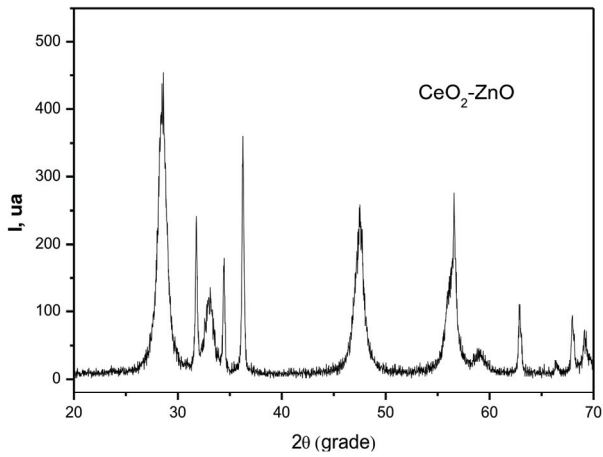


Fig. 4. CeO<sub>2</sub> - ZnO X-ray diffraction pattern

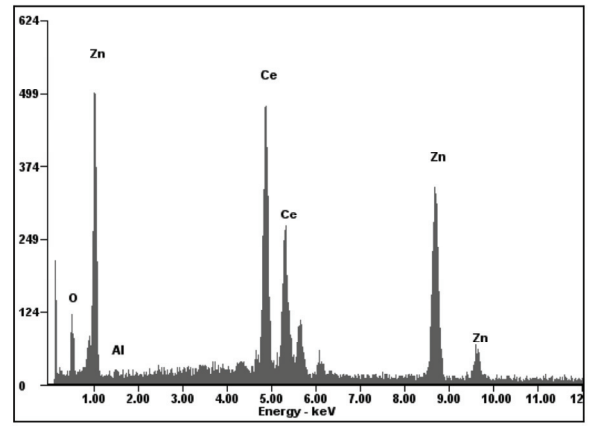


Fig. 5. The EDAX analysis

Table 1. The EDAX analysis

Element	Wt%	At%
O <sub>K</sub>	07.81	32.38
AlK	01.48	03.64
CeL	51.91	24.59
ZnK	38.81	39.40
Matrix	Correction	ZAF

Table 2. The TG – DTA results of CeO<sub>2</sub> - ZnO prepared sample

Stage	T <sub>i</sub>	T <sub>m</sub>	T <sub>f</sub>	w <sub>∞</sub>	DTA
I	30	66	81	1.38	endo
II	81	116	130	9.27	endo
III	130	143	238	7.51	endo
IV	238	270	291	1.17	exo
V	291	332	366	20.42	exo
VI	366	392	415	12.07	exo
VII	415	423	480	1.41	exo
Residue %				46.77	

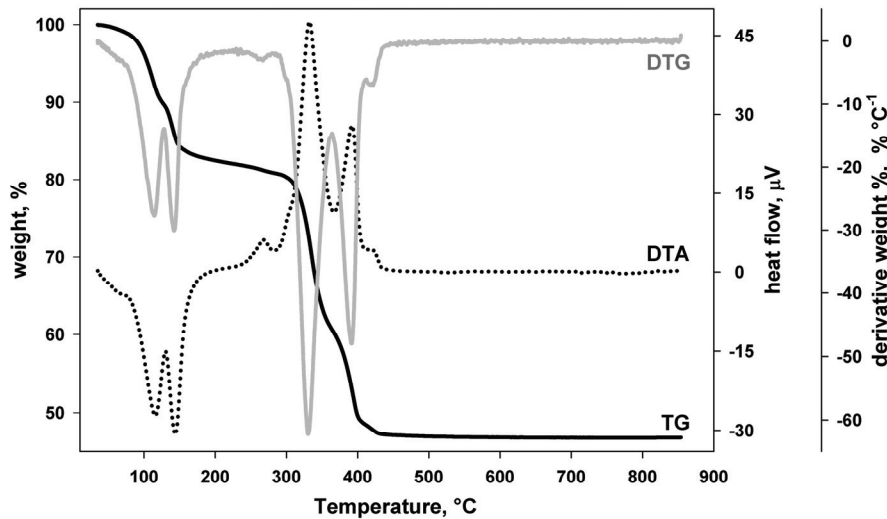
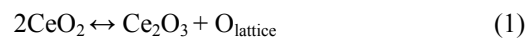


Fig. 6. The TG/DTA curves of CeO<sub>2</sub> - ZnO prepared sample

The catalytic activity of ceria can be related with the oxygen evolution and absorption equilibrium reaction shown in Eqs. (1-2) (Nakatsuji et al., 2013).



#### 4.2. The photocatalytic activity

The photocatalytic activity of CeO<sub>2</sub> - ZnO samples was evaluated by measuring the decomposition rate of MB and PMBH under UV light irradiation. Figs. 7 and 8 show the changes of MB and PMBH concentration with reaction time under UV irradiation and in presence of CeO<sub>2</sub> - ZnO catalyst.

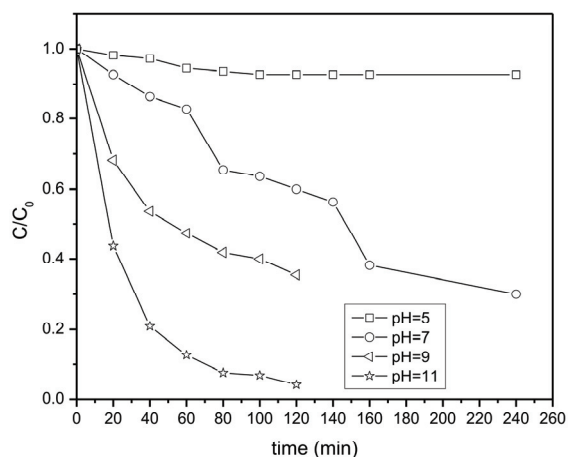
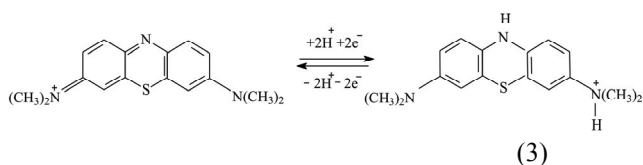


**Fig. 7.** The MB degradation under UV irradiation, initial MB concentration =  $10^{-5}$  mol/L and 0.1 g/L CeO<sub>2</sub> - ZnO

MB degradation was followed for 260 min. In acidic media were not observed changes in the dye behaviour. After about 3 hours, the MB concentration was only slightly smaller than the initial one. At pH = 7, and pH = 9, the degradation of MB was about 60 %, faster result being reached in basic medium. For pH = 11 MB degradation was achieved in 90 % in just 2 hours, which is remarkable considering the intensity of UV radiation used.

The degradation occurs due to the following reaction (Eq. 3):



The photoreduction is reversible and is measured by decoloration ratio, the leucoderivative formed being white due to the breaking of the double bonds at the nitrogen atom. The leucoderivative has an absorption maximum at 225 nm, while the methylene blue has the absorption maximum at 664 nm. The PMBH dye has an azoic structure, thus it acts different from the MB.

PMBH degradation was also followed at different pH values for 300 min. In neutral and acidic media after 150 min were not observed notable changes in analysed system behaviour. In basic medium, after 300 minutes only 30% of the original compound has been degraded. The azo group is a well-known weak group, so it was a surprise result the fact that only 30% of the dye was decomposed.

The high resistance to UV action occurs due to the extended conjugated system and the electrons transitions, but this hypothesis will be further studied using various analytical methods.

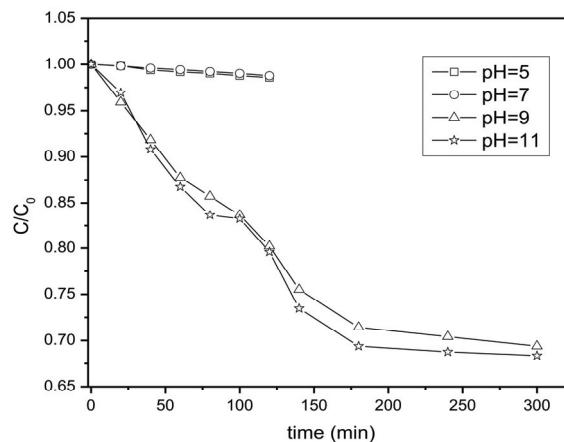


**Fig. 8.** The PMBH degradation under UV irradiation, initial PMBH concentration =  $5 \cdot 10^{-5}$  mol/L and 0.1 g/L CeO<sub>2</sub> - ZnO

#### 5. Conclusions

CeO<sub>2</sub> - ZnO: nanopowder was synthesized by a surfactant-assisted solvo-thermal route. The method is simple and lead to the preparation of ultrafine particles with required characteristics. SEM analysis showed that the particles have spheroidal shape and their sizes range from 50 to 80 nm, which is appropriate for a homogeneous suspension. Moreover, CeO<sub>2</sub> - ZnO systems present photocatalytic activity leading to degradation of two organic substances: MB almost total in basic medium and PMBH less.

#### References

- Abbas M., Parvatheeswara Rao B., Reddy V., Kim C.G., (2014), Fe<sub>3</sub>O<sub>4</sub>/TiO<sub>2</sub> core/shell nanocubes: Single-batch surfactantless synthesis, characterization and efficient catalysts for methylene blue degradation, *Ceramics International*, **40**, 11177–11186.
- Akyol A., Bayramoglu M., (2005), Photocatalytic degradation of Remazol Red F3B using ZnO catalyst, *Journal of Hazardous Materials B*, **124**, 241–246.
- Ameen S., Akhtar M.S., Shin S.H., (2012), Growth and characterization of nanospikes decorated ZnO sheets and their solar cell application, *Chemical Engineering Journal*, **195-196**, 307–313.
- Arsene D., Teodosiu C., Barjoveanu G., Apreutesei R.E., Apopei P., Musteret C.P., Cailean D., (2013), Combined catalytic oxidation and adsorption of priority organic pollutants for wastewater recycling, *Environmental Engineering and Management Journal*, **12**, 907-916.
- Bansal P., Sud D., (2011), Photodegradation of commercial dye, Procion Blue HERD from real textile wastewater using nanocatalysts, *Desalination*, **267**, 244–249.
- Ezenwa I.A., (2012), Synthesis and optical characterization of zinc oxide thin film, *Research Journal of Chemical Sciences*, **2**, 26–30.

- Faisal M., Ismail A.A., Ibrahim A., Bouzid H., Al-Sayari S.A., (2013), Highly efficient photocatalyst based on Ce doped ZnO nanorods: Controllable synthesis and enhanced photocatalytic activity, *Chemical Engineering Journal*, **229**, 225–233.
- Fan D.H., Zhu Y.F., Shen W.Z., Lu J.J., (2008), Synthesis and optical properties of hierarchical pure ZnO nanostructures, *Materials Research Bulletin*, **43**, 3433–3440.
- Ghods F.E., Tepehan F.Z., Tepehan G.G., (2008), Optical and structural properties of sol gel made Ce/Ti/Zr mixed oxide thin films as transparent counter electrode for electrochromic devices, *Optical Materials*, **31**, 63–67.
- Kashif M., Ali M.E., Usman Ali S.M., Hashim U., (2013), Sol-gel synthesis of Pd doped ZnO nanorods for room temperature hydrogen sensing applications, *Ceramics International*, **39**, 6461–6466.
- Khataee A., Karimi A., Arefi-Oskoui S., Soltani R.D.C., Hanifehpour Y., Soltani B., Joo S.W., (2015), Sonochemical synthesis of Pr-doped ZnO nanoparticles for sonocatalytic degradation of Acid Red 17, *Ultrasonics Sonochemistry*, **22**, 371–381.
- Ko H.H., Yang G., Cheng H.Z., Wang M.C., Zhao X.J., (2014), Growth and optical properties of cerium dioxide nanocrystallites prepared by coprecipitation routes, *Ceramics International*, **40**, 4055–4064.
- Kumar P.S., Abhinaya R.V., Arthi V., Gayathri Lashmi K., Priyadharshini M., Sivanesan S., (2014), Adsorption of methylene blue dye onto surface modified cashew nut shell, *Environmental Engineering and Management Journal*, **13**, 545-556
- Lima J.F., Martins R.F., Neri C.R., Serra O.A., (2009), ZnO:CeO<sub>2</sub>-based nanopowders with low catalytic activity as UV absorbers, *Applied Surface Science*, **255**, 9006–9009.
- Nakatsuji T., Kunishige M., Li J., Hashimoto M., Matsuzono Y., (2013), Effect of CeO<sub>2</sub> addition into Pd/Zr–Pr mixed oxide on three-way catalysis and thermal durability, *Catalysis Communications*, **35**, 88–94.
- Nascimento L.F., Martins R.F., Silva R.F., Serra O.A., (2014), Catalytic combustion of soot over ceria-zinc mixed oxides catalysts supported onto cordierite, *Journal of Environmental Sciences*, **26**, 694–701.
- Orbeci C., Nechifor Gh., Stănescu R., (2014), Removing toxic compounds from wastewater, *Environmental Engineering and Management Journal*, **13**, 2153-2158.
- Paul H., Kessler D., Herr U., (2008), Optical properties of nanocrystalline YAG:Ce, *Solid State Phenomena*, **140**, 9-16.
- Preetam S., Hegde M.S., (2008), Controlled synthesis of nanocrystalline CeO<sub>2</sub> and Ce<sub>1-x</sub>M<sub>x</sub>O<sub>2-δ</sub> (M = Zr, Y, Ti, Pr and Fe) solid solutions by the hydrothermal method: Structure and oxygen storage capacity, *Journal of Solid State Chemistry*, **181**, 3248–3256
- Shafaei A., Nikazar M., Arami M., (2010), Photocatalytic degradation of terephthalic acid using titania and zinc oxide photocatalysts: Comparative study, *Desalination*, **252**, 8–16.
- Shidpour R., Simchi A., Ghanbari F., Vossoughi M., (2014), Photo-degradation of organic dye by zinc oxide nanosystems with special defect structure: Effect of the morphology and annealing temperature, *Applied Catalysis A: General*, **472**, 198–204.
- Wang L.S., Xiao M.W., Huang X.J., Wu Y.D., (2009), Synthesis, characterization, and photocatalytic activities of titanate nanotubes surface-decorated by zinc oxide nanoparticles, *Journal of Hazardous Materials*, **161**, 49–54.